Dhaka Univ. J. Sci. 69(3): 149-153, 2022 (June)
Centennial Special Issue

ISSN 1022 - 2502, E-ISSN 2408-8528
DOI: https://doi.org/10.3329/dujs.v69i3.60024

Induced Hyperfine Field in Doped Chalcopyrite Compounds $Cu(In_{1-x}A_x)S_2$ (A = V and Cr)

M. Shahjahan* **and Raisul Islam**

Department of Physics, University of Dhaka, Dhaka 1000, Bangladesh

(Received: 31 October 2021; Accepted: 14 February 2022)

Abstract

Hyperfine field and electronic states of doped chalcopyrite compounds $Cu(In_{1-x}A_x)S_2$ with A = V and Cr are calculated by Korringa-Kohn-Rostoker Green's function method, where x denotes the concentration of A atoms. The V and Cr doped compounds are ferromagnetically stable in terms of energy minimization and their electronic states are half metallic. The hyperfine fields in the stable ferromagnetic (FM) state are calculated with their valence and core contributions. In addition, site preference local magnetic moments are calculated for the FM and disordered spin moment (DSM) states. Density of states (DOS) exhibit the spintronic property of half metallicity. The local core and valence field polarizations are found in the doped chalcopyrite systems, where the *s*-orbital hybridization with the local *d*-shell is explained in terms of some exchange mechanisms.

Keywords: Hyperfine field; KKR-CPA; Magnetic moment; Density of states; Doped chalcopyrite; Core polarization.

I. Introduction

Hyperfine field (HF) is an area of current research, which provides unique microscopic information about dilute ferromagnetic (FM) and antiferromagnetic alloys. A suitable ferromagnetic alloy can be designed with 3*d* transition metal (TM) doping into the host matrix of a semiconductor material. The 3*d* impurities have a local moment in dilute ferromagnets, whereas *s-p* impurities are nonmagnetic. The hyperfine magnetic properties depending on the impurity concentrations are induced by the local core and valence *s*-electrons interaction with the nearest neighbor *d*-shell. The hyperfine energy level shift is contributed by three terms such as Fermi contact, orbital and dipolar terms. Among them the leading contribution to the HF results from the term of Fermi contact interaction, which is obtained by the densities of spin magnetization m(r = 0) at the nucleus[1].

Recently, Blügel et al. calculated HF of 3*d* and 4*d* impurities in nickel (Ni) elements. Their formed alloys are binary type using the elements of 3*d* and 4*d* series, where the hyperfine properties in the semi-relativistic approximation are calculated for three different exchange-correlation potentials[1]. Akai et al. have performed self-consistent calculations of alloys formed by TM impurities and light interstitials in elemental iron (Fe) for finding HF[2]. Korhonen et al. attempted to find HF in bcc Fe with heavy impurities using a full-potential approach of Korringa-Kohn-Rostoker Green's function (KKR-GF) method[3]. The Banerjee group reported the TDPAC (time differential perturbed γ-γ angular correlation) measurements in HfO_2. They studied hyperfine interaction in pure and Gd-doped HfO_2 and attributed it to three orthorhombic crystal phase[4]. The Lee-Hone group calculated magnetic structure and the distribution of transferred HF at the Sn site of the rare-earth element (R) based RMgSn compounds[5]. At room temperature (RT), the host matrix of copper indium sulfide, $CuInS_2$ (CIS) is a moderately gapped semiconductor with body centered tetragonal structure, having a couple of cations and lone anion sites. The transition from nonmagnetic to magnetic material is occurred by hosting 3*d* impurities at either or both of the cation sites of the host CIS compound[6].

In this study, magnetic hyperfine properties of doped chalcopyrite compounds $Cu(In_{1-x}A_x)S_2$ are investigated using the KKR-GF method, where A is the impurity atoms (V, Cr) and x denotes the low concentration of A atom. The V and Cr are two consecutive TM atoms having d^2 and d^3 electron configurations, which are used as dopants to understand the relative strength of induced HF at V and Cr sites. The TM atoms are substituted at the cation site of In^{3+} rather than Cu^{1+} due to the stability of the system in terms of the minimum energy. There were a few attempts to calculate HF in ternary compounds by introducing 3*d* TM and some other atoms[7-9]. The hyperfine interactions in the $Bi_{1-x}La_xFeO_3$ ferrites, HF at Mn site in the intermetallic compound $LaMnSi_2$, and magnetic interactions and different magnetic properties in $Fe_{1-x}M_xSb_2O_4$, M = Mg, Co, were investigated by the research groups of Pokatilov[7], Domienikan[8], and Berry[9], respectively. We have been motivated to find hyperfine interactions and various induced hyperfine magnetic properties in a relatively large alloy system. Therefore, introducing of TM atoms at In^{3+} cation site of CIS matrix show a phase transition from semiconductor to FM state and yield local moments and dominating core polarized Fermi contact HF. The net magnetic moment (NM) is directly proportional to the Cr concentrations in doped CIS matrix. The induced properties originate from the inner zone of the atoms near the nucleus. The role of doped impurities on magnetic hyperfine properties is discussed, since in FM materials and their alloys the significant hyperfine quantity is directly related to the spin density m(r = 0) at the nucleus. The HF of both the impurity and the nearest neighbor atoms are estimated in terms of the relativistic corrections and therefore the orbital contribution term is neglected in the calculations[10, 3].

*Author for correspondence. e-mail: mjahan@du.ac.bd

The layout of the article is as follows: computational methods and scopes are termed briefly in section II. The NM, spin magnetic moments (SM), total and component DOS of doped CIS compounds and hyperfine magnetic properties are presented in tabular form and graphically and explained them in section III. In section IV, the concluding remarks on results are described.

II. Computational Scope

Hyperfine interactions of doped chalcopyrite compounds $Cu(In_{1-x}A_x)S_2$ with A = V and Cr are calculated with the self-consistent KKR-GF band structure method[11]. The technique of CPA (coherent potential approximation) is used for handling the fractional impurity mixed to the pure system[12]. The SRA (scalar relativistic approximation) is implemented in the calculation to accommodate the relativistic effects. The generalized gradient approximation (GGA) by Perdew, Burke and Ernzerhof is used for the estimation of the exchange correlation (XC) energy functional of the doped CIS systems[13]. The muffin-tin (MT) type perturbed potential approximation is attributed for shaping the form of the potential, since the MT zero potential is determined by the host system and cannot be changed near the impurity. The electronic charge density, wave functions, and the crystal potential are expanded in terms of spherical harmonics inside the MT spheres with radii R_{MT} centered at the nuclear positions. The angular momenta $\ell = 2$ is taken into account to specify the spherical harmonics for the electronic wave functions. To calculate HF accurately, the total-energy difference between the magnetic states is taken up to the sixth decimal place of the Rydberg scale. The experimental band gap of CIS is 1.53 eV. The experimental lattice parameters (ELP) for CIS, a = 5.52 Å, c = 11.13Å, and inner parameter u = 0.214 are used for the numerical calculations[14]. The hyperfine magnetic properties of the doped CIS compounds are calculated by the ELP of pure CIS compound. Almost 145 k sampling points of the first Brillouin zone (BZ) is considered to carry out the BZ integration. Employing the CPA technique, the doped CIS compounds are calculated by the program package 'Machikaneyama' based on KKR-CPA developed by Akai[15].

III. Results and Discussion

In the calculation of hyperfine properties of doped chalcopyrite compounds $Cu(In_{1-x}A_x)S_2$, the relativistic corrections are significant for heavy nuclei with relatively large nuclear charges. Because, the hyperfine fields are essentially determined from the wave functions near the nucleus by employing the contact interaction formula. The calculated magnetic moments of Cr doped CIS matrix such as NM for each unit cell and SM for each magnetic ions in terms of doping concentrations are shown in Figs.1(a, b). The presented filled circles and squares are the calculated data and the connecting fitted lines indicate the overall trend of the moments. The NM is directly proportional to the concentrations, whereas the SM is slowly falling down with concentrations.

The site preference local SM per atom and net HF are tabulated in Table 1 for 5% concentrations of V and Cr doped CIS compounds. The zero SM results at the nonmagnetic atomic sites, where a small amount of HF is induced by orbital hybridization. A nonzero HF is obtained at Cu, In, and S sites even though no NM is induced. The field strength is around 40% stronger at Cr site compared to V site.The up and down arrow indicate the spin disordered system of the corresponding FM configuration, where zero net SM and zero net HF is obtained owing to the cancellation of up spin and down spin electronic states[16]. Therefore, the vector sum of the induced magnetic moments and HF both at host and doped atomic sites is zero. Relatively larger values of SM and HF are obtained in Cr doped CIS compounds rather than V doped cases due to a preferential occupation of the high-spin states of Cr d^3 electronic configuration.

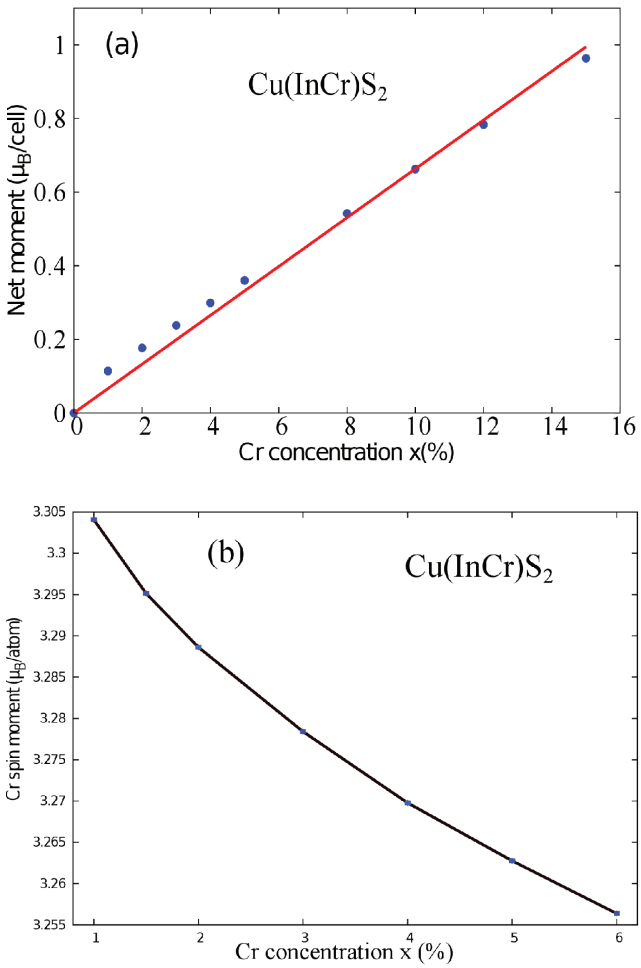

Fig. 1. Calculated (a) total magnetic moments (NM) for each unit cell and (b) local spin moments (SM) for each atom (in Bohr magneton) of Cr doped CIS compound as a function of Cr concentrations. The filled circles and squares represent the calculated results connected with the fitted solid lines.

Table 1. Induced local spin moments (SM) in μ_B/ion and total hyperfine fields (HF) in KG/ion of $Cu(In_{1-x}A_x)S_2$ with 5% concentrations of A = V and Cr at In^{3+} cation site in FM and DSM configurations. Listed data with physical units clarify the variances of induced fields and moments at different sites.

Composition : Unit	Cu site	In site	A site	S site
$Cu(In_{0.95}V_{0.05})S_2$: μ_B /ion	0	0	2.25	0
$Cu(In_{0.95}V_{0.05})S_2$: KG/ion	5.24	27.7	−162.51	1.86
$Cu(In_{0.95}V^{\uparrow}_{0.025}V^{\downarrow}_{0.025})S_2$: μ_B /ion	0	0	±2.24	0
$Cu(In_{0.95}V^{\uparrow}_{0.025}V^{\downarrow}_{0.025})S_2$: KG/ion	0	0	±162.82	0
$Cu(In_{0.95}Cr_{0.05})S_2$: μ_B /ion	0	0	3.26	0
$Cu(In_{0.95}Cr_{0.05})S_2$: KG/ion	7.1	22.66	−226.48	1.89
$Cu(In_{0.95}Cr^{\uparrow}_{0.025}Cr^{\downarrow}_{0.025})S_2$: μ_B /ion	0	0	±3.26	0
$Cu(In_{0.95}Cr^{\uparrow}_{0.025}Cr^{\downarrow}_{0.025})S_2$: KG/ion	0	0	±227.92	0

The NM for each unit cell and SM for each Cr atom along with valence, core and net HF are displayed in Table 2 for doping of 1% to 6% Cr in CIS compound. The values of NM significantly change with Cr concentrations, whereas SM seems to be steady with Cr concentrations. However, the core and valence HF are oppositely polarized and therefore, the net HF are aligned to the core course. The overall trend of HF is related to SM and thus slowly falling down with increasing impurity concentrations. The calculated hyperfine magnetic properties are found to be in reasonable agreement with other reported values[1, 2]. In the calculation of HF, both the orbital and dipolar field contributions are neglected because of their minor corrections to the presented results.

Table 2. Net moments (NM), local spin moments (SM) and hyperfine fields (HF) for Cr impurity doping at In^{3+} cation site of $CuInS_2$, where HF^c is the core contribution, HF^v is the valence one and $HF^t = HF^c + HF^v$ is the total value of fields in KG.

Composition	NM (μ_B/cell)	SM (μ_B/Cr)	HF^c (KG/Cr)	HF^v(KG/Cr)	HF^t (KG/Cr)
$Cu(In_{0.99}Cr_{0.01})S_2$	0.12	3.30	−395.48	165.67	−229.81
$Cu(In_{0.98}Cr_{0.02})S_2$	0.18	3.29	−393.67	165.33	−228.35
$Cu(In_{0.97}Cr_{0.03})S_2$	0.25	3.28	−392.47	164.98	−227.49
$Cu(In_{0.96}Cr_{0.04})S_2$	0.31	3.27	−391.44	164.56	−226.88
$Cu(In_{0.95}Cr_{0.05})S_2$	0.37	3.26	−390.58	164.09	−226.48
$Cu(In_{0.94}Cr_{0.06})S_2$	0.43	3.26	−389.79	163.57	−226.22

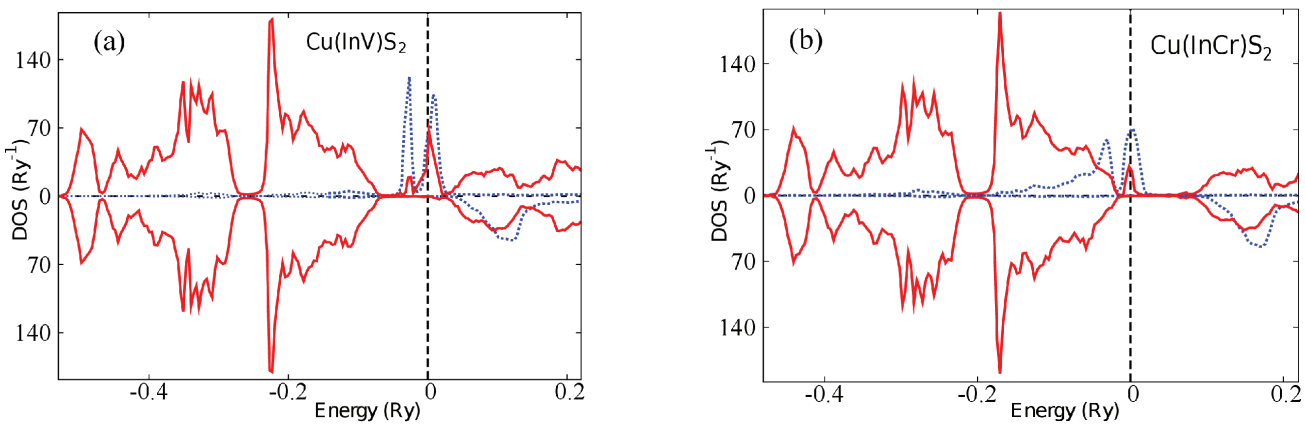

Fig. 2. Total density of states (DOS) for each unit cell (solid line) of (a) $Cu(InV)S_2$ and (b) $Cu(InCr)S_2$ compounds for 5% concentrations of TM atoms. Dotted line indicates the component DOS for 3*d* states of V and Cr atoms, respectively. The upper and lower panels specify the spin up and spin down densities, orderly. The Fermi energy level is denoted by a vertical dashed line, which is set at $E_F = 0$ Ry.

The total and component DOS of V and Cr doped CIS compounds for 5% concentrations are shown in Figs. 2(a, b) in a wide energy interval of energy axis around the Fermi energy level at $E_F = 0$ Ry, where the states beyond the Fermi level are empty. The valence states are interacting and hybridizing around the Fermi level. Therefore, the DOS exhibits spin bands lying around the Fermi energy level only in up spin direction with no spin states at the down spin direction. The full spin polarization indicates the half metallic situation at the Fermi energy level and therefore induces NM, SM and HF. The spin polarized component DOS, split because of the crystal-field perturbation, are responsible for spin band varying around the Fermi level and producing FM properties in the doped CIS compounds[17–19].

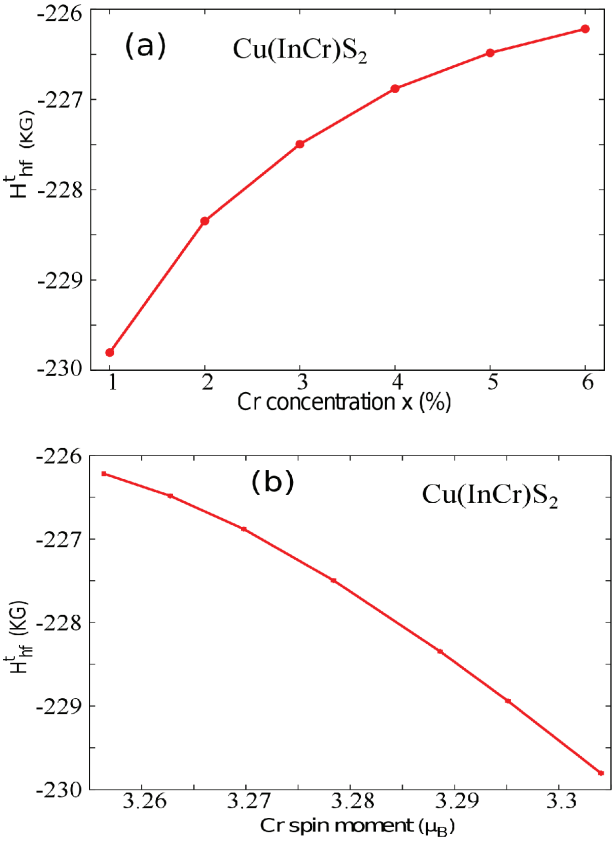

Fig. 3. The trend of core polarized total hyperfine fields in KG with (a) impurity concentrations and (b) local spin moments of Cr doping at In^{3+} cation site of CIS compound. The filled circles and squares represent the calculated results connected with the fitted solid lines.

The HF originates from the spin polarized charge density at the nuclear position. The contributory terms for HF are contact field, orbital field and spin-dipolar field[20]. The trend of net HF in KG with Cr concentrations and SM are shown in Figs. 3(a, b), where the semi-core states are included within the contour of energy and therefore considering them as valence states. The polarization of In 5*p* subshells is attributed to their hybridization with extended spin-polarized valence states. The fact that the total core polarization is always opposite in sign to the local moments, whereas the valence polarization is in the same sign to SM. Since, the relativistic corrections are relatively trivial for the 3*d* atoms (usually 10% for the TM impurities), therefore in the calculations semi-relativistic approximation is considered. The spin band coupling is enhanced by Cr doping and dominates the variant magnetic properties of the system. The changes of the valence-*d* and core-*s* wave functions through the TM atoms are responsible for this variation[1, 2].

IV. Conclusions

Induced hyperfine properties of chalcopyrite compounds with V and Cr transition-metal impurities are presented by *ab-initio* calculations, where the collinear magnetization axes of V and Cr are considered. The correct treatment of core, semi-core and valence electrons of the impurity atoms are taken in the calculation of HF and local moments. The values of the local magnetic moments and HF at the atomic sites are estimated from the Fermi contact hyperfine interactions. A large core negative HF is obtained, which is proportionate to the local moments. On the contrary, a positive local valence field is found, which is directly proportional to the local moments. The *s-d* exchange mechanism leads to the induced core polarization over the valence one, where the majority spin-density of *s*-state electrons near the nucleus is mainly caused by the contact interaction.

Acknowledgment

The authors are grateful to the authority of the University of Dhaka for providing partial support by the centennial research grant (CRG).

References

1. Blügel, S., H. Akai, R. Zeller and P. H. Dederichs, 1987. Hyperfine Fields of 3*d* and 4*d* Impurities in Nickel. *Phys. Rev.* B. **35 (7),** 3271–3283.

2. Akai, M, H. Akai and J. Kanamori, 1987. Electronic Structure of Impurities in Ferromagnetic Iron. III. Light Interstitials. *J. Phys. Soc. Jpn.* **56 (3),** 1064–1077.

3. Korhonen, T., A. Settels, N. Papanikolaou, R. Zeller and P. H. Dederichs, 2000. Lattice Relaxations and Hyperfine Fields of Heavy Impurities in Fe. *Phys. Rev. B.* **62 (1)**, 452–460.

4. Banerjee, D., C. C. Dey, Sk. W. Raja, R. Sewak, S. V. Thakare, R. Acharya and P. K. Pujari, 2019. Stability of Monoclinic Phase in Pure and Gd-Doped HfO_2: a Hyperfine Interaction Study. *Hyperfine Interact* **240**, 78–85.

5. Lee-Hone, N. R., P. Lemoine, D. H. Ryan, B. Malaman, A. Vernière and G. Le Caër, 2014. Calculating the Distribution of Transferred Hyperfine Fields at the Sn Site in Tetragonal CeScSi-Type RMgSn Compounds. *Hyperfine Interact* **226**, 309–319.

6. Shahjahan, M., M. Toyoda and T. Oguchi, 2014. Ferromagnetic Half Metallicity in Doped Chalcopyrite Semiconductors $Cu(Al_{1-x}A_x)Se_2$ (A =3d Transition-Metal Atoms). *J. Phys. Soc. Jpn.* **83**, 094702–094706.

7. Pokatilov, V. S., D. A. Salamatin, A. V. Bokov, A. V. Salamatin, A. Velichkov, M. V. Mikhin, D. S. Grozdov, K. N. Vergel, A. S. Sigov, A. O. Makarova, M. Budzynski and A. V. Tsvyashchenko, 2021. Hyperfine Interactions in the $Bi_{1-x}La_xFeO_3$ Ferrites (x = 0.0225, 0.075, 0.9). *Hyperfine Interact* **242***,* 33–42.

8. Domienikan, C., B. Bosch-Santos, G. A. Cabrera Pasca, R. N. Saxena and A. W. Carbonari, 2015. Hyperfine Field at Mn in the Intermetallic Compound $LaMnSi_2$ Measured by PAC Using ^{111}Cd Nuclear Probe. *Hyperfine Interact* **231,** 95–99.

9. Berry, F. J., B. P. de Laune, C. Greaves, H-Y Hah, C. E. Johnson, J. A. Johnson, S. Kamali, J. F. Marco, M. F. Thomas and M. J. Whitaker, 2018. Magnetic Interactions in $Fe_{1-x}M_xSb_2O_4$, M = Mg, Co, Deduced from Mössbauer Spectroscopy. *Hyperfine Interact* **239***,* 31–38.

10. Breit, G, 1930. Possible Effects of Nuclear Spin on X-ray Terms. *Phys. Rev.* **35***,* 1447–1451.

11. Kohn, W. and N. Rostoker, 1954. Solution of the Schrödinger Equation in Periodic Lattices with an Application to Metallic Lithium. *Phys. Rev.* **94 (5),** 1111–1120.

12. Shiba, H., 1971. A Reformulation of the Coherent Potential Approximation and its Applications. *Prog. Theor. Phys.* **46 (1),** 77–94.

13. Perdew, J. P., K. Burke and M. Ernzerhof, 1996. Generalized Gradient Approximation Made Simple. *Phys. Rev. Lett. 77 **(18)**, 3865–3868.*

14. Abrahams, S. C. and J. L. Bernstein, 1973. Piezoelectric Nonlinear Optic $CuGaS_2$ and $CuInS_2$ Crystal Structure: Sublattice Distortion in $A^IB^{III}C_2^{VI}$ and $A^{II}B^{IV}C_2^{V}$ Type Chalcopyrites. *J. Chem. Phys.* **59 (10),** 5415–5422.

15. Akai, H., 2002. <http://kkr.issp.u-tokyo.ac.jp/>

16. Schröter, M., H. Ebert, H. Akai, P. Entel, E. Hoffmann and G. G. Reddy, 1995. First-Principles Investigations of Atomic Disorder Effects on Magnetic and Structural Instabilities in Transition-Metal Alloys. *Phys. Rev. B* **52 (1),** 188–209.

17. Wolf, S. A., D. D. Awschalom, R. A. Buhrman, J. M. Daughton, S. von Molnár, M. L. Roukes, A. Y. Chtchelkanova and D. M. Treger, 2001. Spintronics: a Spin-Based Electronics Vision for the Future. *Science* **294 (5546),** 1488–1495.

18. Ohno, H., 1998. Making Nonmagnetic Semiconductors Ferromagnetic. *Science* **281 (5379),** 951–956.

19. Lin, H. -F., W. -M. Lau and J. Zhao, 2017. Magnetism in the p-Type Monolayer II-VI Semiconductors SrS and SrSe. *Sci. Rep.* **7 (1),** 1–10.

20. Lalić, M. V., J. Mestnik-Filho, A. W. Carbonari, R. N. Saxena, and H. Haas, 2001. First-Principles Calculations of Hyperfine Fields in the $CeIn_3$ Intermetallic Compound. *Phys. Rev. B* **65 (5),** 054405–054411.